

RESEARCH ARTICLE

Overall dynamic body acceleration measures activity differently on large versus small aquatic animals

Lucía Martina Martín López^{1,2}  | Natacha Aguilar de Soto³ | Peter T. Madsen⁴ | Mark Johnson^{4,5}

¹School of Environmental Sciences, University of Liverpool, Liverpool, UK

²Ipar Perspective Asociación, Karabiondo Kalea, Sopela, Spain

³BIOECOMAC, Department of Animal Biology, Edaphology and Geology, University of La Laguna, Tenerife, Spain

⁴Zoophysiology, Department of Biology, Aarhus University, Aarhus, Denmark

⁵Aarhus Institute of Advanced Studies, Aarhus University, Aarhus, Denmark

Correspondence

Lucía Martina Martín López
Email: luciamartinaml@gmail.com

Mark Johnson
Email: markjohnson@bios.au.dk

Handling Editor: Luca Börger

Abstract

1. Acceleration-based proxies for activity and energy expenditure are widely used in bio-logging studies of animal movement and locomotion to explore biomechanical strategies, energetic costs of behaviour, habitat use and the impact of anthropogenic disturbance. The foremost such proxy is overall dynamic body acceleration (ODBA) along with variants VeDBA and PDBA. This technique, which involves summing the magnitude of high-pass-filtered acceleration signals (the so-called dynamic acceleration) over a reference interval, has been applied to animals as diverse as shags, lobsters, humans and whales. The relationship between ODBA and energy use has been tested empirically on animals small enough to house in laboratory facilities and arguments have been offered for why the method should be generally applicable; however, validations on larger animals are scant.
2. Here, we examine how body size impacts ODBA and its variants under steady locomotion in large aquatic animals, using cetaceans as model species. To do this, we first develop a simplified mathematical model for the acceleration signals that would be measured by a tag on a swimming animal. We then test this model with empirical data gathered using bio-logging tags on whale species spanning 1.3 m harbour porpoises to 12-m sperm whales.
3. We show that the motions measured by ODBA can be fundamentally different in small versus large aquatic animals. Whereas dynamic acceleration in small animals is predominantly due to specific acceleration (i.e. actual accelerative motions generated by muscle action), in larger aquatic animals, body rotations (i.e. cyclical angular displacements associated with swimming) can dominate the measured acceleration.
4. As body rotations do not necessarily increase in magnitude as swimming speed increases, ODBA may underestimate the relative cost of behaviours or responses to disturbance in large aquatic animals. This does not lessen the value of ODBA for small animals, but it raises a caution against uncritical use on larger animals. For large aquatic animals, activity proxies that specifically remove body rotations

This is an open access article under the terms of the Creative Commons Attribution-NonCommercial License, which permits use, distribution and reproduction in any medium, provided the original work is properly cited and is not used for commercial purposes.

© 2021 The Authors. *Methods in Ecology and Evolution* published by John Wiley & Sons Ltd on behalf of British Ecological Society.

using gyroscopes or magnetometers may provide more consistent estimates of energy use although these methods are yet to be validated.

KEYWORDS

aquatic locomotion, cetaceans, dynamic acceleration, energy expenditure, ODBA, postural dynamics, scaling, specific acceleration

1 | INTRODUCTION

Understanding the kinematics and costs of locomotion is fundamental to unravelling how animals exploit resources and resolve life-history trade-offs, as well as in assessing the potential costs of disturbance. Early insights into locomotion in terrestrial, aerial and aquatic animals were obtained using cinematographic recording of animals on treadmills (Taylor et al., 1970) in wind tunnels (Tucker, 1970) or water flumes (Schmidt-Nielsen, 1972). In addition to providing high-resolution data on full body movement, these captive test environments offered the possibility of also measuring forces, cardiac rate and oxygen consumption at a range of locomotion speeds. This resulted in energetics models that account for both the mechanical power expended and the metabolic power required at different levels of steady activity (Schmidt-Wellenburg et al., 2008; Williams, 1999). However, the limited size of test facilities precludes larger animals and even experiments with smaller animals must be often performed under conditions with little ecological relevance.

An alternative approach has been to instrument animals with bio-logging devices and these have provided a range of insights into the fine-scale biomechanics and behaviour of free-ranging fauna (Brown et al., 2013). High-resolution archival tags containing sensors such as pressure, speed and triaxial accelerometers and magnetometers have been deployed on many terrestrial and aerial species but have been especially valuable for aquatic animals such as cetaceans that spend most of the time underwater (Brown et al., 2013). A major area of research interest has been to infer the energetic cost of animal activities from accelerometer data. Accelerometers measure mass-specific force via Newton's second law, $f = ma$. As work (i.e. energy) is the integral over time of the product of force and speed, there is a direct link between acceleration and the mass-specific mechanical work done by an animal, at least with respect to the movements that reach the tag (Gleiss, Wilson, et al., 2011). Based on this, Wilson et al. (2006) developed a proxy for energy expenditure termed the overall dynamic body acceleration (ODBA) defined as the sum over a reference interval of the magnitude of the triaxial acceleration after the removal of a running mean.

Although other proxies for activity and energetics have been proposed, ODBA and its variants are by far the most widely used methods. A number of studies have demonstrated a clear individual-specific relationship between oxygen consumption (VO_2) and ODBA, showing that ODBA can be used as a proxy for energy expenditure during the tested activities on the tested species (Wilson

et al., 2020). An important caveat is that acceleration-based proxies only quantify mechanical energy use and cannot account directly for metabolic energy consumed by physiological processes such as thermoregulation (Gleiss, Wilson, et al., 2011). Concerns have also been raised about potential errors resulting from a so-called time-trap involving the trivial correlation of increasing functions of time (Halsey, 2017; Ladds, et al., 2017), but this can be avoided by dividing ODBA by the observation duration, resulting in a mean activity measure rather than an accumulating one. However, despite some testing effort, the reliability of ODBA as a measure of mechanical energy expenditure remains largely unknown when extrapolated to individuals of different size, ontogenetic state or species, as well as to different behaviours, locomotory modes and tag placements (Gleiss et al., 2010; Wilson et al., 2020).

A recent effort to address this uncertainty (Byrnes et al., 2021) demonstrated a body mass scaling effect on the VO_2 -ODBA relationship for smaller (max. 17 kg) animals highlighting the importance of validating ODBA under representative conditions. However, validation is a major challenge for large animals that cannot be studied in a captive setting, and yet are increasingly targeted for bio-logging studies of energy expenditure as a function of natural and disturbed behaviour. But, even though the relationship between ODBA and VO_2 may be unknown for such large animals, ODBA could be a useful relative measure of energy use provided it is consistent, that is, if a change in energy expenditure in movement results in a comparable relative change in ODBA. Such consistency has been argued at a theoretical level (Wilson et al., 2020) and is implicitly assumed in studies that compare the relative cost of activities (Gleiss et al., 2010; Gleiss, Jorgensen, et al., 2011; Gleiss, Norman, et al., 2011), but has not been verified on large animals. Here, we test the consistency of ODBA as a mechanical energy measure on toothed whale species that cover an order of magnitude difference in body length. We show that this assumption is not borne out for large aquatic animals because ODBA may measure a fundamentally different aspect of movement in large animals than it does for small animals. On small animals, ODBA largely measures muscle-generated acceleration making it an effective proxy for mechanical work, but for aquatic animals bigger than about 3 m, ODBA can also be influenced by the body rotations generated by locomotion which may not scale consistently with energy use. To show this, we first consider what animal-attached accelerometers actually measure during locomotion and develop a simple mathematical model for ODBA. We then compare the predictions from this model to recordings from bio-logging tags on small and large cetaceans.

2 | ACCELERATION MEASUREMENTS ON ANIMALS

Animal-attached accelerometers are sensitive to both the orientation of the animal via gravity and acceleration generated by non-isometric muscle action. This latter component is termed the specific force acceleration or just the specific acceleration (SA) in the strapdown inertial navigation literature (Savage, 1998) and is directly linked to energy use in animals as muscles consume energy to contract and so generate acceleration (Gleiss, Wilson, et al., 2011). Even though acceleration is typically measured with a bio-logging tag attached to a single location on the body, muscle contractions throughout the body give rise to accelerations that are coupled to the tag, to greater or lesser extent, through the body frame. Thus, single-point acceleration measurements can be an effective tool for monitoring activity. Metabolic energy may also be expended in maintaining and changing orientation (e.g. through isometric or slow muscle contractions), but the relationship between orientation and energy use is complex and indirect. For example, in aquatic animals, a statically extended fin similar to the rudder of a boat may cause a continual turning movement, but the energetic cost of this may not be easily inferred from the changing orientation. Consequently, the most direct information about mechanical energy expenditure is conveyed by the SA, but to characterise this component of the accelerometer signal, it is first necessary to remove the orientation component.

The beautiful simple idea behind ODBA is to use a filter to attenuate the orientation component. This recognises that, compared to the speed of muscle contractions, animals generally change orientation slowly due to rotational inertia. Thus, filtering the acceleration data with an appropriately chosen high-pass filter reduces the magnitude of the orientation term while leaving the SA largely unaffected (Shepard et al., 2008). The high-pass-filtered triaxial acceleration is termed the dynamic acceleration, DA, although this term has also been used interchangeably with SA in some papers on the assumption that the filtering is fully effective at removing the orientation component (e.g. Shepard et al., 2008; Shiomi et al., 2010; Williams et al., 2017). However, the distinction between these two terms is important for mathematical analysis and we therefore propose the following definitions to resolve the ambiguity in the literature: SA is the actual muscle-generated acceleration that we wish to measure in order to infer energetics; DA is the signal resulting from filtering the on-animal acceleration measurements and so contains both the SA and any remnant orientation component. In effect, SA is a hidden state within the DA and the two terms are equal only if the filtering completely removes the orientation (i.e. gravitational) component.

In the Wilson et al. (2006) definition of ODBA, the high-pass filter is implemented in two steps: first, a centralised moving average (MA) is computed on each axis and the outputs of this are then subtracted from the original acceleration. This scheme is efficient to compute on a low-power microprocessor such as may be used in a bio-logging tag. However, it results in a filter frequency response that has varying sensitivity in the passband and that attenuates relatively weakly

at low frequencies. We recommend the use of a longer symmetric finite impulse response (FIR) high-pass filter that has the advantages of a flatter passband response and increased attenuation of lower frequencies at the expense of more computation (see Figure S1 in Supporting Information).

Whichever filter is used, the cut-off frequency (i.e. the frequency above which signals are passed largely unattenuated) should be selected so as to pass most of the SA and little of the orientation-related acceleration signal. For active animals, locomotion represents a major energy expense and typically involves the largest muscles in the body. As muscle contraction speed is inversely related to fibre length (Medler, 2002), locomotion muscles tend to generate the lowest frequency components in the SA. It therefore seems logical to set the high-pass filter cut-off frequency at some fraction of the dominant locomotory rate (e.g. the stride rate in terrestrial animals, wingbeat rate in birds and the stroke rate in swimmers). Based on acceleration data during steady swimming in several marine vertebrates, Shepard et al. (2008) suggest an MA of 3 s or at least one locomotory stroke cycle whichever is longer, equating to a filter half-power frequency of 0.15 Hz or lower. Such a low cut-off frequency results in ODBA being sensitive to orientation changes in small agile animals. To avoid this, we suggest that the cut-off frequency be set at a consistent fraction (e.g. in the range 40%–60%) of the dominant stroke cycle frequency of each subject (see Figure S1 in Supporting Information for more details on the filter design issues).

The final step in ODBA involves computing the magnitude of the triaxial DA which is then summed over the desired interval. Variants of ODBA differ in the way that the magnitude is calculated. In ODBA, the magnitude is taken as the sum of the absolute value of each axis. This may lead to an overestimation of acceleration in some circumstances (Gleiss et al., 2009) leading to the proposal of Vectorial Dynamic Body Acceleration (VeDBA) in which the usual vector magnitude (i.e. the square-root of the sum of the squares) is used (Gleiss, Wilson, et al., 2011). VeDBA has the advantage of being insensitive to the orientation of the tag on the animal (Qasem et al., 2012) but otherwise gives largely comparable results to ODBA (Wilson et al., 2020). Another variant, the partial dynamic body acceleration (PDBA, Halsey et al., 2009), uses a subset of the accelerometer axes but follows the same computational steps of a high-pass filter followed by magnitude computation and summation.

A critical assumption underpinning ODBA and its variants is that animal orientation changes slowly compared to the frequencies of costly muscle contractions that produce SA (Gleiss et al., 2010). However, for many animals, the movement of extremities during locomotion induces cyclic changes in body posture. This is most readily visualised in the propulsive wave which passes down the body of swimming fish and marine mammals (Lindsey, 1978). Swimmers using body and caudal undulations are broadly classified according to how far this induced body rotation (i.e. cyclical angular displacement of the body associated with swimming, see the glossary and Supporting Information for further explanations of this term) reaches anteriorly (Lighthill, 1971)

from anguilliform (large rotations throughout the body length) to thunniform (rotations that decrease strongly anteriorly). Thus, the instantaneous orientation component in the acceleration reflects both the overall posture of the animal (i.e. slowly varying postural changes such as a change of dive angle or a banking turn) and the smaller cyclical angular displacements of the body that are inevitable during locomotion (Martín López et al., 2016; Shepard et al., 2008). As these latter body rotations occur at the same frequency as SA, that is, at the locomotory rate, they contribute an oscillatory term to the acceleration that cannot be separated from SA by filtering and are therefore included in ODBA. We call this added oscillatory acceleration due to locomotory body rotations the dynamic orientation acceleration (DOA, see the glossary). The DA is therefore the sum of the SA (from muscle contractions) and the DOA (from cyclic orientation changes in locomotion), and these two constituent terms cannot be separated without resorting to additional information, for example, from a sensor such as a gyroscope that is sensitive to orientation but not SA. Although we focus here on undulating movements in aquatic swimming, terrestrial locomotion also often involves small body rotations at the stride rate (Kilbourne & Hoffman, 2013) meaning that in many taxa, the DA contains a combination of muscle action and orientation signals.

The presence of DOA in the measured acceleration complicates the relationship between ODBA and energy expenditure because the DOA and SA components in ODBA vary with locomotion effort in different ways. For example, an animal that increases its stroking rate for the same propulsor extension generally also increases its energy expenditure but, as we confirm below, a higher stroke rate results in an increased SA but not an increased magnitude of the DOA. This does not imply that the body rotations have no associated energetic cost, but the cost cannot be inferred from the magnitude of the orientation component in the measured acceleration. The problem can be resolved by using an additional sensor, either a gyroscope (Ware et al., 2016) or magnetometer (Martín López et al., 2016), to provide an independent estimate of the body rotations which can then be removed from the measured acceleration, that is, yielding an estimate of SA. However, both sensors have drawbacks: Gyroscopes consume significant power, while the magnetometer method is restricted to locomotion styles that involve rotations around a single axis (Martín López et al., 2016).

The approach taken in developing ODBA as an energy proxy is to assume that the body rotations are small and so have a negligible contribution (Gleiss, Wilson, et al., 2011) and this may often be a reasonable assumption. However, even small body rotations can generate substantial accelerations when multiplied by the gravitational acceleration (9.8 m/s^2) to produce the DOA. Thus, it is important to determine under what conditions the body rotations can really be ignored, and the DA can be taken as an accurate measure of the SA. As a step towards answering this, we develop in the following a simplified mathematical model to assess the relative magnitude of the SA and body rotation contributions to ODBA in swimming locomotion.

3 | MODEL PREDICTIONS

For many active predators, a large proportion of the energetic costs that can be captured by an accelerometer are incurred in locomotion. For example, in aquatic air-breathing animals diving to forage, the cost of transport between two disparate resources, air at the surface and prey at depth, will often dominate the mechanical costs. To examine how body size impacts ODBA-style metrics under steady locomotion, we build on a simplified model proposed by Simon et al. (2012) for the acceleration signals measured by a tag attached to the skin of a swimming animal:

$$A_t = Q_t G + S_t, \quad (1)$$

where $A_t = [a_{x_t}, a_{y_t}, a_{z_t}]^T$ is the triaxial measured acceleration at time t (the superscript T means the transpose of a vector or matrix); Q_t is a rotation matrix that defines the instantaneous orientation of the body surface where the tag is attached; G is the gravity vector, that is, $[0, 0, g]^T$ in a {north, east, up} frame with $g = 9.81 \text{ m/s}^2$; $S_t = [s_{x_t}, s_{y_t}, s_{z_t}]^T$ is a vector representing the net SA of the body surface at the tag location, where s_{x_t} , s_{y_t} and s_{z_t} are the surge, sway and heave SA respectively. We assume that the tag sensors are calibrated and that their axes (x, y, z) are aligned with the longitudinal, transverse and ventral–dorsal axes of the animal, or that the data are corrected to reflect the measurement that would have been made with an aligned tag (Johnson & Tyack, 2003). The model in Equation 1 is simplified in that centrifugal acceleration due to body rotations is neglected, but this will normally have a much smaller magnitude than the SA for the small rotations considered here (it may not be negligible, however, on a soaring or stooping bird; Clark, 2009). The model also neglects acceleration transients, for example, from striking at prey, as we are focusing on steady locomotion. Extraneous high-frequency acceleration noise, such as induced by water flow around the tag (Cade et al., 2018), is also neglected in this simplified model. For tags that are attached to an animal elastically (e.g. with suction cups), a low-pass filter or decimation operation may be advisable to reduce the magnitude of such exogenous noise before computation of ODBA. The need for, and design of, this filter is discussed in the Supporting Information.

Overall dynamic body acceleration and variants are calculated by high-pass filtering A_t to produce the dynamic acceleration, DA, and then summing the magnitude of this vector over a time interval. Our goal is therefore to assess how much each component in Equation 1 contributes to the magnitude of DA.

We consider animals that swim by planar movements of a caudal propulsor. For simplicity, we consider just the case of horizontal swimming and vertical swimming (e.g. during a steep dive descent or ascent) and assume that the animal is in a dorsal side up orientation (i.e. is not rolled to one side). Under these assumptions, the gravitational term in Equation 1 can be replaced with:

$$Q_t G = D_t P G, \quad (2)$$

where $P = \begin{pmatrix} \cos(p) & 0 & \sin(p) \\ 0 & 1 & 0 \\ -\sin(p) & 0 & \cos(p) \end{pmatrix}$ is a rotation matrix accounting for the

mean orientation of the animal and p is the mean pitch angle. D_t is a time-varying rotation matrix that accounts for body rotations in swimming. Together, P and D_t represent the instantaneous orientation Q_t of the animal. For animals, such as cetaceans, that swim with a dorsoventral propulsor action:

$$D_t = \begin{pmatrix} \cos(r_t) & 0 & \sin(r_t) \\ 0 & 1 & 0 \\ -\sin(r_t) & 0 & \cos(r_t) \end{pmatrix}, \text{ where } r_t \text{ is the time-varying pitch}$$

angle (in radians) with respect to the mean pitch of the body at the tag position (Martín López et al., 2015). For animals such as phocid seals and fish that use transversal propulsor movements:

$$D_t = \begin{pmatrix} \cos(r_t) & \sin(r_t) & 0 \\ -\sin(r_t) & \cos(r_t) & 0 \\ 0 & 0 & 1 \end{pmatrix},$$

where r_t is now a time-varying sway angle. For simple sinusoidal propulsor movement, $r_t \approx \alpha \sin(2\pi f_s t)$, where α is the peak rotation angle in radians with respect to the mean during a propulsive stroke at the tag location, and f_s is the stroking rate in Hz. For thunniform swimming, α is small (e.g. $<10^\circ$ for cetaceans) allowing us to make the approximations: $\cos(r_t) \approx 1$ and $\sin(r_t) \approx r_t$ in both forms of propulsion. Thus, D_t becomes:

$$D_t \approx I + r_t \begin{pmatrix} 0 & 0 & 1 \\ 0 & 0 & 0 \\ -1 & 0 & 0 \end{pmatrix} \text{ for dorso - ventral propulsion,}$$

$$D_t \approx I + r_t \begin{pmatrix} 0 & 1 & 0 \\ -1 & 0 & 0 \\ 0 & 0 & 0 \end{pmatrix} \text{ for transverse propulsion,}$$

where I is the 3×3 identity matrix. Substituting these approximations into the gravitational acceleration formula, Equation 2, gives:

$$Q_t G \approx g [\sin(p) \ 0 \ \cos(p)]^T + g r_t [\cos(p) \ 0 \ -\sin(p)]^T \text{ for dorso - ventral propulsion,}$$

$$Q_t G \approx g [\sin(p) \ 0 \ \cos(p)]^T + g r_t [0 \ -\sin(p) \ 0]^T \text{ for transverse propulsion.}$$

Applying a high-pass filter to these equations gives the dynamic orientation acceleration, DOA. A well-designed high-pass filter (HPF) should remove the static terms in these equations but leave the term involving r_t intact because this varies at the stroking rate, that is:

$$\text{DOA} = \text{HPF} \{Q_t G\} \approx g r_t [\cos(p) \ 0 \ -\sin(p)]^T \text{ for dorso - ventral propulsion,}$$

$$\text{DOA} = \text{HPF} \{Q_t G\} \approx g r_t [0 \ -\sin(p) \ 0]^T \text{ for transverse propulsion.}$$

The magnitude $\| \cdot \|$ of DOA is therefore approximately:

$$\| \text{DOA} \| \approx g \alpha \text{ for dorso - ventral propulsion,} \quad (3a)$$

$$\| \text{DOA} \| \approx g \alpha \sin(|p|) \text{ for transverse propulsion.} \quad (3b)$$

For simplicity, the magnitude here is taken as the peak positive value. If the mean-absolute-value (as in ODBA) or the Root-Mean-Squared (RMS, as in VeDBA) were used, these equations would have an additional constant multiplier of 0.636 or 0.707, respectively, for sinusoidal motion but as the same constant will also appear below in the magnitude of SA, it can be ignored.

Turning now to the SA term in Equation 1, caudal propulsion generates SA in both the longitudinal axis of the animal (i.e. surge SA) and in the axis perpendicular to the direction of travel in which the propulsor moves. For dorsoventral propulsion, this is a heave SA (i.e. SA in the dorsoventral axis) while for transverse propulsion, it is a sway SA (SA in the lateral axis). In steady cetacean swimming, we have found that the surge SA is proportional to, but is typically less than or equal to, the heave SA (Martín López et al., 2015), and the same likely applies to the sway SA in transverse propulsion. The heave or sway SA is more readily modelled mathematically, and we therefore assume that they are representative of the total SA. For each swimming style, the body displacement in the heave or sway axis for sinusoidal propulsor movement is $d \sin(2\pi f_s t)$ where d is the peak up/down or sideways body displacement at the tag location. The body displacement may be offset in phase with respect to the body rotation by an amount that depends on the swimming style and tag location, but this can be ignored as we are only concerned with the relative magnitudes of these components. The heave or sway SA is the double differential of the body displacement, that is, $-4\pi^2 f_s^2 d \sin(2\pi f_s t)$. The high-pass filter used in computing the DA passes this signal unaffected because it varies at the stroking rate. Thus, the magnitude of the SA component in the DA for both types of propulsion is approximately:

$$\| \text{SA} \| \approx 4\pi^2 f_s^2 d. \quad (4)$$

The approximation is due to the assumption of simple sinusoidal body movement and because we have neglected the contribution of the surge

SA. The dynamic acceleration is the vector sum of the specific and dynamic orientation acceleration components so $\| (\| \text{DOA} \| - \| \text{SA} \|) \| \leq \| \text{DA} \| \leq (\| \text{DOA} \| + \| \text{SA} \|)$ by the triangle inequality. Therefore, if one of $\| \text{SA} \|$ or $\| \text{DOA} \|$ is significantly larger than the other, the $\| \text{DA} \|$ will closely follow

that dominant component. As ODBA and VeDBA are just scaled sums of $\|DA\|$ over specific time intervals, the same is true of these activity proxies.

In this simplified locomotion model, the $\|DOA\|$ is approximately equal to $g\alpha$ for dorsoventral propulsion but varies with pitch angle for transverse propulsion reaching a maximum of $g\alpha$ when the animals are descending or ascending vertically. Comparing this to Equation 4, $\|SA\|$ will be at least twice as large as $\|DOA\|$ and so dominate ODBA if:

$$2\pi^2 f_s^2 d \gtrsim g\alpha \quad \text{for dorso-ventral propulsion,} \quad (5a)$$

$$2\pi^2 f_s^2 \gtrsim g\alpha \sin(|p|) \quad \text{for transverse propulsion.} \quad (5b)$$

As $g \approx \pi^2$, the inequality of Equation 5a is met if:

$$f_s \gtrsim \sqrt{(\alpha/2d)}. \quad (6)$$

To assess under what circumstances this is true, we need to consider the likely values of f_s , d and α , which are, respectively, the stroking rate (in Hz), the perpendicular displacement amplitude (m) and the rotation amplitude (radians) at the tag location on the body. Both d and α depend on where the tag is attached to the body and are expected to increase monotonically with distance from the centre of rotation (Fish, 2002). Although there are few data to draw from in the literature, a simplified model for body motion during stroking (see Supporting Information) suggests that d and α should increase at about the same rate as the measurement position is moved caudally. If this is a reasonable approximation, the constraint on f_s in Equation 6 should be roughly independent of tag location on the body. The same model suggests that d may increase proportionally more than α for anterior tag positions due to the stiffness of the thoracic/abdominal vertebral column in many swimming animals. But the square-root in the inequality of Equation 6 likely makes f_s relatively insensitive to tag location.

However, body length, BL, has an important influence on f_s and d . For a given swimming style, for example, thunniform, and assuming that the tag is placed at the same relative location on the body α should be fairly independent of BL because of the geometric similarity of the motion. Conversely, d should be proportional to BL for geometrically similar swimming movements and f_s has been shown to be approximately inversely proportional to BL for a wide range of swimming seabirds and marine mammals (Sato et al., 2007). Thus, our simplified model for heave acceleration in steady swimming predicts that the SA contribution to DA decreases with increasing BL while the DOA contribution to DA, that is, the part due to body rotation during locomotion, is independent of BL for a given swimming style. For the largest cetaceans, the stroking rate appears to decrease more slowly with BL (Gough et al., 2019) suggesting that $\|SA\|$ may reach an asymptote rather than continuing to decrease as BL increases. However, due to the low stroking rate of these massive animals, the asymptotic value of $\|SA\|$ is almost certainly well below the typical values of $\|DOA\|$.

SA is therefore most likely to dominate ODBA or VeDBA in animals with high stroking rates. In contrast, for large enough animals, ODBA and VeDBA will be dominated by the acceleration due

to body rotations, DOA, and will be therefore largely insensitive to changes in stroking rate (unless these are accompanied by a change in stroking amplitude) because $\|DOA\|$ is independent of the stroking rate. These activity measures may thus fail to capture fully the relationship between transport cost and swimming speed in large animals. In the following section, we use empirical results to define rough body size limits below which ODBA provides a reasonable estimate of the SA.

An additional prediction resulting from Equation 5b is that for animals such as phocid seals with transverse propulsion, DOA is only significant during steep descent or ascent swimming. During horizontal swimming, body rotations, and therefore DOA, do not contribute to the acceleration because the rotation occurs in a plane that is orthogonal to the gravity vector. This means that ODBA and VeDBA measure different aspects of motion depending on the orientation of the animal making it problematic to compare the apparent activity level of larger animals in different parts of dives.

4 | EMPIRICAL MEASUREMENTS

The simplified mathematical model above makes a number of assumptions about cetacean swimming which require validation with empirical data. As the model makes specific predictions about how acceleration components vary with body length, we chose validation data from three toothed whale species that cover an order of magnitude difference in lengths but appear to have similar swimming styles. The empirical dataset (Martín López et al., 2021) is comprised of body movements during steady swimming recorded using suction cup attached multi-sensor tags (DTAGs version 2 and 3) on *Phocoena phocoena* harbour porpoises (Pp), *Mesoplodon densirostris* Blainville's beaked whales (Md) and *Physeter macrocephalus* sperm whales (Pm). Tags were attached to sperm whales ($n = 6$) between 2003 and 2010 in Norway, Italy, the U.S. North Atlantic and the Azores using a cantilevered pole mounted to the bow of a small rigid hulled inflatable boat (Miller et al., 2004). Blainville's beaked whales ($n = 6$) were tagged between 2003 and 2010 off the coast of El Hierro (Canary Islands, Spain) using a handheld pole from a small inflatable boat (Johnson et al., 2004). Harbour porpoises ($n = 6$) were bycaught in a pound net fishery in inner Danish waters between 2012 and 2014 and tagged upon release (Wisniewska et al., 2016). Tags were positioned just behind the blowhole on Pp, and between the dorsal fin and blowhole on Md and Pm. In all cases, the tags released autonomously to float at the surface and were recovered using radio tracking. See Supporting Information for the specific ethics permits under which the cetacean tagging was conducted. The tags included a pressure sensor, triaxial magnetometers and triaxial accelerometers sampled at 50–200 Hz with 16-bit resolution. These sensor streams were decimated to a common 25-Hz sampling rate in post processing (i.e. by applying an anti-alias filter to the raw sensor data and then downsampling to a common 25-Hz sampling rate). This decimation serves both to standardise the sampling rates and to remove high-frequency vibration from water flow (Cade et al., 2018). The triaxial

accelerometer and magnetometer signals were rotated to correct for the orientation of the tag on the whale which was estimated at each surfacing from the stereotypical movements during respiration (Johnson & Tyack, 2003). Software tools from www.animaltags.org in Matlab R2019a (Mathworks Inc.) were used for data processing.

The tagged animals performed periods of continuous strokes during the ascent phase of dives. For each animal, 10 randomly selected data blocks of 10 consecutive swimming strokes were analysed. A cut-off frequency of 0.4 of the dominant stroke cycle frequency was used to separate the DA from the lower frequency orientation postural signals. The body rotations as well as the DOA and SA components in the DA were estimated separately using the magnetometer method (Martín López et al., 2016). Body length (Table S1 in Supporting Information) was measured in Pp but was estimated from visual observations for Md and Pm.

As a specific example, the body rotations recorded on a harbour porpoise and on a sperm whale with similar anterior tag locations had closely similar magnitude (RMS of 4.7° and 3.9° for Pp and Pm, respectively), while the RMS heave and surge SAs were around 10 and 12 times bigger, respectively, for the porpoise compared to the sperm whale (RMS heave and surge SA for Pp: 2.7 and 1.9 m/s²; and for Pm: 0.26 and 0.11 m/s²; Figure 1).

Results for all 18 animals (Figure 2) confirm that, while SA decreases sharply with increasing body length (due to decreasing fluking rate), the contribution of body rotations, via DOA, to the dynamic acceleration, and therefore ODBA remains roughly constant. The intraspecies variation in these motion parameters in Pp, Md and Pm is likely due to the variable tag locations on the body rather than differences in individual swimming style. In fact, body rotations are less variable across species than within species (Table S1) supporting the expectation that body rotations are independent of body size

for similar relative tag placements. But notwithstanding these measurement artefacts, it is evident that body rotations, as predicted, constitute a greater proportion of the DA in larger animals such as sperm whales. In comparison, for small animals such as harbour porpoises, the acceleration is dominated by the SA to the extent that DA and SA can be considered interchangeable during steady swimming. Fitting the model predictions for $\|DOA\|$ and $\|SA\|$ to the species means in Figure 2 and applying the relationship between stroke rate and body length from Sato et al. (2007) suggest that SA dominates (i.e. is at least twice the magnitude of DOA) for body lengths less than about 3 m.

To assess more specifically the relative magnitude of SA and DOA, we evaluated the inequality in Equation 5 using estimates of the stroking rate (f_s , in Hz), the perpendicular displacement amplitude (d , in m) and the body rotation amplitude (α , in radians) for one individual of each species. During horizontal swimming, the dorso-ventral displacement experienced by the tag as the propulsive wave travels along the body shows up as a cyclical variation in pressure, allowing us to estimate d from the high-pass filtered depth. We estimated d , α and f_s during 10 periods of 10 consecutive strokes of near-horizontal swimming at the tag location on the body of a harbour porpoise (Pp), a Blainville's beaked whale (Md) and a sperm whale (Pm) (Table S2 in Supporting Information). Body rotations were roughly constant across species (4.5, 6.3 and 5.7 0-to-peak degrees, for Pp, Md and Pm respectively), suggesting that tags were attached at comparable relative positions on the bodies. As predicted, stroking rate decreased with increasing body length ($f_s = 1.5$, 0.44 and 0.17 Hz for Pp, Md and Pm respectively), while body displacement increased with increasing body length ($d = 1.6$, 20.0 and 25.2 cm for Pp, Md and Pm respectively). The stroking rate was approximately equal to $\sqrt{(\alpha/2d)}$ for the harbour porpoise but was slightly smaller

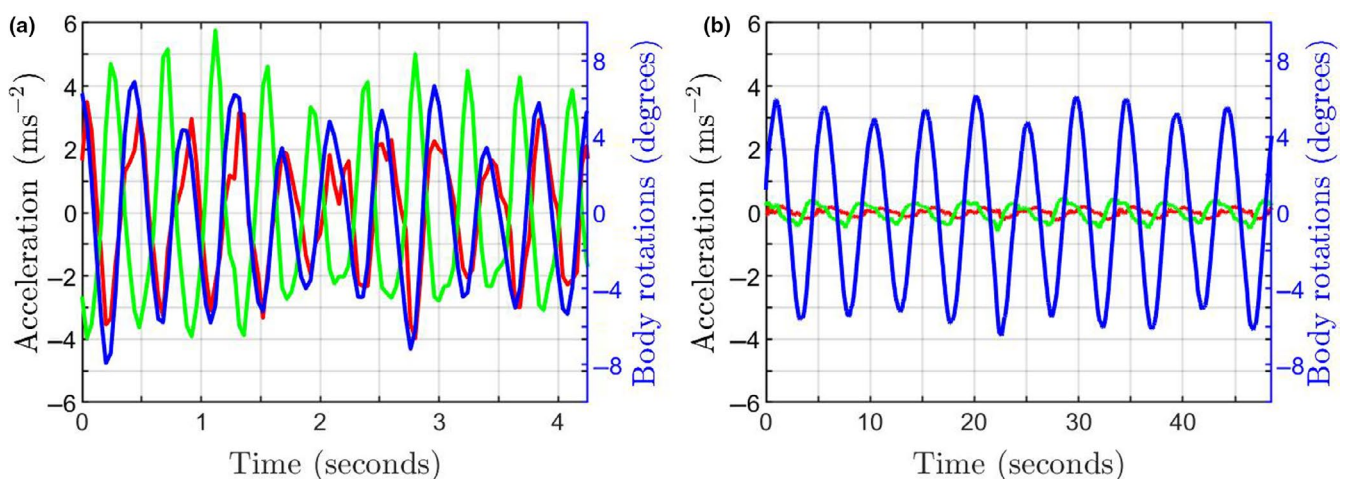


FIGURE 1 Comparison of estimated heave and surge specific acceleration (SA, green and red lines, respectively) and body rotations (blue) during 10 consecutive swimming strokes recorded on two cetacean species with a similar tag location: (a) Harbour porpoise with a stroke cycle frequency of 2.4 Hz (a 4.3-s interval is shown); (b) Sperm whale with a stroke cycle frequency of 0.21 Hz (48.5 s interval). Note the similar magnitude of body rotations despite the extreme body size difference of these two species (approximately 1.3 m vs. 13 m), whereas both SA components are much smaller in the sperm whale compared to the porpoise

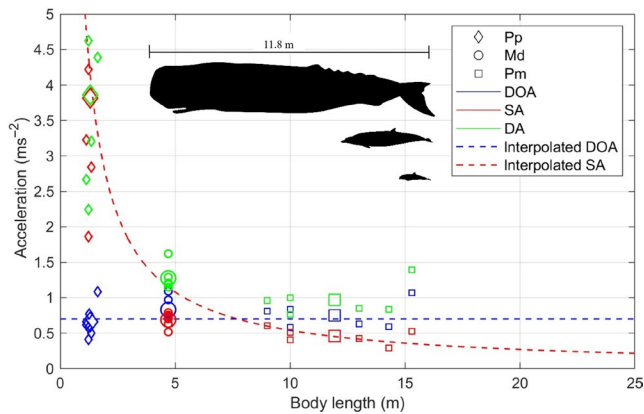


FIGURE 2 Measured and interpolated acceleration components during locomotion as a function of body length for cetacean swimming. Empirical data are taken from suction cup-attached tags on six sperm whales (Pm, squares), six Blainville's beaked whales (Md, circles) and six harbour porpoise (Pp, diamonds). Small points show the mean values of the RMS dynamic acceleration (DA, green), specific acceleration (SA, red) and dynamic orientation acceleration (DOA, blue) during continuous swimming for each individual. Body lengths were measured, estimated or inferred from the literature (see Table S1 in Supporting Information). Large data points indicate the species average. Theoretical interpolations for $||DOA||$ (dashed blue line) and $||SA||$ (dashed red line) were obtained by fitting Equations 3a and 4 to the species averages using the relationship between body length and fluking rate for steady swimming from Sato et al. (2007). DA cannot be predicted without knowing the phase lag between accelerations and rotations for the swimming style and tag location on the body; however, the magnitude of DA will be slightly greater than the larger of $||DOA||$ and $||SA||$ matching the empirical measurements (green points). Silhouettes made by Dr. Alina Loth (<http://www.engagedart.uk/>)

than this critical value for a Blainville's beaked whale and considerably smaller for a sperm whale.

5 | DISCUSSION

Quantifying how animals expend energy through activity is a major goal of bio-logging and reliable measurements would improve our understanding of the efficiency with which animals perform vital activities and allow for quantification of the potential costs of human disturbance. Due to the complexity of animal movement, estimates of energy use from single tags are unlikely to be accurate (Wilson et al., 2020) but are nonetheless useful provided they are consistent, that is, if an increase in activity results in a corresponding increase in the proxy. ODBA is by far the most widely used energy metric, and is supported by a number of empirical studies showing a strong relationship with metabolic energy use (Wilson et al., 2020). However, a theoretical basis for this metric is lacking beyond the basic physical relationship between muscle force production and acceleration (Gleiss, Wilson, et al., 2011).

A core assumption underlying ODBA is that acceleration contributions from orientation and muscle contractions have different

frequency contents and so can be separated by filtering (Gleiss, Wilson, et al., 2011). Although Shepard et al. (2008) acknowledge that body rotations may occur at the same frequency as muscle contractions during locomotion, they argue that the impact of this dynamic orientation acceleration (DOA) signal on ODBA is small. Here, we tested that assertion for swimming animals using both mathematical modelling and empirical measurements. Our analysis confirms that ODBA and its variants offer a useful proxy for mechanical energy in relatively small aquatic animals by quantifying, within the limitations of a single-point measurement, the SA generated by muscle contractions. For these small animals, the measured dynamic acceleration (DA) is a close estimate of the SA justifying the interchangeable usage of these terms in some papers. However, we show that swimming motions in larger animals typically generate low specific accelerations and that body rotations can contribute a gravitational acceleration signal to the DA which is comparable or larger than the SA. On these larger animals, the DA may not track the SA closely and ODBA may therefore not provide a consistent proxy for mechanical energy. We demonstrate this with cetacean swimming, but the conclusion may apply to other locomotion styles. The conclusion also applies to variants of ODBA such as VeDBA and PDBA which use the same basic processing steps.

Swimming, like other forms of locomotion, involves a complicated array of synchronous muscle movements and the model developed here relies on a number of simplifying assumptions to be tractable. Nonetheless, comparison of the model predictions with empirical measurements on three species spanning a 10:1 size range demonstrates that the model captures the fundamental relationships between body length and skin surface acceleration in swimming. The model offers several predictions about how well ODBA quantifies changing locomotion effort in swimmers which we examine in the following.

For swimmers that use body and caudal undulation for propulsion, the magnitude of body rotations in locomotion varies with stroke amplitude but not stroking rate. Although swimmers may modulate either stroke amplitude or rate to meet changing locomotion needs, the additional drag associated with large propulsor extensions may make stroke rate the more efficient way to adjust swimming output (Saadat et al., 2017). If this is the case for the larger animals for which body rotations, via the DOA, dominate the dynamic acceleration, ODBA will be insensitive to changes in locomotion effort making it unreliable as a proxy for energy use for these animals. A particular situation in which this could give misleading results is in behavioural response studies on large tagged whales (Tyack et al., 2011) in which it may be logical to compare locomotor output during intervals with and without disturbance. If animals are swimming in both experimental conditions but swim with a higher stroke rate during exposure, this may be only weakly evident in the ODBA.

A similar inconsistency applies to large aquatic animals such as phocid seals and sharks with transverse propulsion. In these animals, the motion quantified by ODBA varies with the pitch angle: in horizontal swimming, ODBA tracks SA accurately, but in vertical swimming, DOA may exceed SA leading to a changing relationship between ODBA and locomotion effort. This orientation-dependent

relationship matters when comparing the relative energetic cost of behaviours that are performed with different pitch angles, for example, in deep-divers such as elephant seals that spend a considerable part of each dive in near-vertical swimming (Le Boeuf et al., 1992). Conversely, for sharks that rarely ascend or descend at steep angles (Andrzejczek et al., 2020; Gleiss, Norman, et al., 2011), the problem may be less pronounced.

Given the potential for misinterpretation of ODBA on large aquatic animals, a key question is at which body size do these problems become manifest. Although this depends on the locomotion style, and so may be difficult to predict in general, a rough rule of thumb can be arrived at from Equation 5 for swimming animals. For ODBA to be dominated by the SA, as intended in its formulation, the $\|SA\|$ should be $\gtrsim 2\|DOA\|$ and this is the case, under our simple swimming model, if the stroking rate f_s , is $\gtrsim \sqrt{\alpha/2d}$. Estimating these parameters in the three species, we found that the inequality was nearly met by a 1.1 m harbour porpoise but was missed by a large margin in a 10-m sperm whale. For the Blainville's beaked whale with an approximate body length of 5 m, the SA and DOA have similar magnitudes and so ODBA will be influenced by both aspects of motion and will also be sensitive to the phase between the SA and body rotations as this determines the magnitude of the dynamic acceleration when the components are closely matched. For these mid-sized animals, the relationship between ODBA and mechanical energy may therefore change with stroking rate and gait potentially making comparisons across different gaits unreliable (Martín López et al., 2015). Thus, for aquatic animals larger than about 3 m, such as large pinnipeds and many cetaceans, ODBA may increasingly reflect the body rotations produced in swimming rather than the SA for which it is intended to be a proxy.

This conclusion highlights the potential for misleading results when comparing energetics over individuals of different body sizes within a population, for example, when comparing ODBA between mum-calf pairs. The increased contribution of DOA to ODBA in larger animals may lead to an overestimation of their cost of transport relative to smaller animals. Extrapolation of any acceleration-based energy proxy to larger animals for which validation is not possible should therefore be treated with caution. It is less clear whether similar cautions apply to terrestrial animals. Although walking and running generate both SA and body rotations, SA may not decrease as steeply with increasing body size in terrestrial animals due to the need to oppose gravitational forces when lifting limbs (Alexander, 2003).

The concerns about ODBA on large animals beg the question of whether there may be more universal proxies for energy expenditure in movement. The fundamental issue is the contribution of body rotations to on-animal acceleration that cannot be removed by high-pass filtering. The minimum specific acceleration (MSA) introduced by Simon et al. (2012) avoids sensitivity to body rotations by exploiting the constant magnitude of the orientation component in the acceleration vector. However, this method is sensitive to calibration errors and can only give an underestimate of the SA rather than

a central trend making it more difficult to interpret. An alternative approach is to predict and subtract the DA component in the acceleration vector using an independent sensor, leaving an estimate of the SA. Methods to do this have been proposed using gyroscopes (Kawabata et al., 2014; Martín López et al., 2016; Ware et al., 2016) or magnetometers (Martín López et al., 2016). An ODBA-like energy proxy can then be derived by summing the magnitude of the estimated SA over an interval resulting in the so-called APBA (averaged propulsive body acceleration, Ware et al., 2016) or OSA (overall specific acceleration, Martín López et al., 2016). Although these proxies should, by design, provide consistent measures of mechanical energy over different body sizes, neither method has been validated against an independent energy metric as has been done for ODBA. Moreover, for the large animals in which these alternative methods are most useful, the greater magnitude of DOA relative to SA means that the DOA must be estimated with high accuracy to achieve moderate accuracy in SA. As the estimation accuracy of these methods has yet to be established, it is unclear for what size range of animals they may be beneficial. An additional practical drawback of gyroscopes is that they consume significantly more power than does an accelerometer, reducing the recording time of a bio-logging tag or increasing its size due to larger batteries.

Thus, despite the fundamental importance of measuring energy expenditure in free-living animals, a universal solution is elusive. By sensing mass-specific force, animal-attached accelerometers seem to hold the promise of quantifying mechanical energy use, but their sensitivity to orientation confounds this. While the impact of orientation is minor in small animals, we have shown that it can dominate the acceleration signal in large animals. As a result, ODBA and variants, which are computed from acceleration, can measure fundamentally different aspects of movement in small and large animals, at least in marine fauna. This highlights the need for caution when applying proxies for energetics on species or in behaviours that cannot be independently validated.

6 | GLOSSARY OF TERMS AND ACRONYMS

APBA	Averaged propulsive body acceleration (ms^{-2}); an activity and energy proxy defined in Ware et al. (2016) as the average gain in speed per propulsive stroke divided by mean stroke cycle duration
BL	Body length (m)
Body rotations	Cyclical angular displacements associated with swimming. In steady swimming, this is the rotation angle between the average (i.e. smoothed) body posture and the instantaneous body posture at the tag location. For cetaceans and sirenians, the rotation is largely around the lateral axis (i.e. a pitching rotation) whereas for pinnipeds and fish with caudal propulsion, it is around the dorsoventral axis (a sway rotation)

DA	Dynamic acceleration (ms^{-2}); the measured triaxial acceleration after being filtered by a high-pass filter. The DA contains contributions from the SA and DOA. Note that some authors use DA to refer to the actual muscle-generated acceleration (which we term SA here). We draw a distinction between SA and DA to allow us to test how closely the measurable DA matches the SA (which cannot be directly measured)
DOA	Dynamic orientation acceleration (ms^{-2}); the component in the dynamic acceleration due to body rotations at or above the locomotory rate. The DOA is the remaining gravitational acceleration component in the measured acceleration after filtering with a high-pass filter to produce the DA
DSF	Dominant stroke frequency (Hz); the typical or average locomotory rate of an individual animal (Sato et al., 2007)
FIR	Finite impulse response; a type of filter in which a fixed number of input samples are used to compute each output point
HPF	High-pass filter; a filter that passes signals with frequencies above the filter cut-off frequency and attenuates lower frequency components
MA	Moving average filter; a symmetric finite impulse response filter with a rectangular impulse response
MSA	Minimum specific acceleration (ms^{-2}); an under-bound on the specific acceleration computed from the measured acceleration, defined in Simon et al. (2012). If the acceleration is in ms^{-2} , $\text{MSA} = \lfloor \ A\ - 9.8 \rfloor$
Md	<i>Mesoplodon densirostris</i> (Blainville's beaked whale)
ODBA	Overall dynamic body acceleration (ms^{-2}); the sum of the DA magnitude over a reference interval used as an activity and energy proxy, defined in Wilson et al. (2006). The magnitude is computed as the sum over the three acceleration axes of the absolute value of each axis
OSA	Overall specific acceleration (ms^{-2}); the sum of the SA magnitude over a reference interval used as an activity and energy proxy, defined in Martín López et al. (2016). The magnitude is computed as the square root of the sum of the squares of the three acceleration axes
PDBA	Partial dynamic body acceleration (ms^{-2}); An activity and energy proxy, defined in the same way as ODBA but using a subset of the three axes, defined in Halsey et al. (2009)
Pm	<i>Physeter macrocephalus</i> (sperm whale)
Pp	<i>Phocoena phocoena</i> (harbour porpoise)
SA	Specific acceleration; the net acceleration of the animal due to actual movement (ms^{-2}). Also called the specific force acceleration or the platform acceleration
VeDBA	Vectorial dynamic body acceleration (ms^{-2}); the sum of the DA magnitude over a reference interval used as an activity and energy proxy, defined in Gleiss, Wilson et al. (2011). The magnitude is computed as the square root of the sum of the squares of the three acceleration axes

ACKNOWLEDGEMENTS

We thank all researchers involved in data collection. Thanks to C. Botelho de Oliveira and P. Tyack for sperm whale data, and J. Teilmann and D. Wisniewska for porpoise data. F. Fish and A. Biewener provided helpful advice. We thank the reviewers and handling editor for insightful critique. Data collection in the Canary Islands was funded by the Office of Naval Research (ONR), the National Oceanographic Partnership Program and the Spanish Ministry of Science (CGL2009-13112). Data collection in the Ligurian sea and Gulf of Mexico was funded by ONR, and by the Minerals Management Service Cooperative Agreements 1435-01-02-CA-85186 and NA87RJ0445 under grant #N00014-99-1-0819. Data collection in Andenes was funded by the Carlsberg Foundation, ONR and by the Strategic Environmental Research Development Program. Work in Azores was funded by the Danish Research Council, the Carlsberg Foundation, Fundação para a Ciência e a Tecnologia and Fundo Regional da Ciência, Tecnologia (TRACE-PTDC/MAR/74071/2006 and MAPCET-M2.1.2/F/012/2011). L.M.M.L. was funded by the St. Andrews University Knowledge and Exchange Impact Program. N.A.d.S. was funded by a Ramón y Cajal Fellowship from the Spanish Government. M.J. was supported by the Aarhus University Research Foundation and the EU H2020 Research and Innovation Programme under Marie Skłodowska-Curie grant 754513. Data collection in Kattegat, Denmark was funded by the German Federal Agency for Nature Conservation under contracts 5330/2010/14 and BfN -Cluster 7 'Effects of underwater noise on marine vertebrates'.

CONFLICT OF INTEREST

None of the authors have a conflict of interest.

AUTHORS' CONTRIBUTIONS

M.J. and L.M.M.L. conceived the ideas and designed methodology; M.J., N.A.d.S., L.M.M.L. and P.T.M. collected the data; L.M.M.L. analysed the data; M.J. and L.M.M.L. interpreted the data; M.J. and L.M.M.L. led the writing of the manuscript. All authors contributed critically to the drafts and gave final approval for publication.


PEER REVIEW

The peer review history for this article is available at <https://publons.com/publon/10.1111/2041-210X.13751>.

DATA AVAILABILITY STATEMENT

Data for this paper are deposited in the Dryad Digital Repository <https://doi.org/10.5061/dryad.ns1rn8prc> (Martín López et al., 2021).

ORCID

Lucía Martina Martín López  <https://orcid.org/0000-0003-2984-8606>

REFERENCES

Alexander, R. M. (2003). *Principles of animal locomotion*. Princeton University Press. Retrieved from <http://www.amazon.co.jp/Principles-Animal-Locomotion-McNeill-Alexander/dp/0691086788>

- Andrzejczek, S., Gleiss, A. C., Lear, K. O., Pattiaratchi, C., Chapple, T. K., & Meekan, M. G. (2020). Depth-dependent dive kinematics suggest cost-efficient foraging strategies by tiger sharks: Tiger shark dive kinematics. *Royal Society Open Science*, 7(8). <https://doi.org/10.1098/rsos.200789>
- Brown, D. D., Kays, R., Wikelski, M., Wilson, R. P., & Klimley, A. P. (2013). Observing the unwatchable through acceleration logging of animal behavior. *Animal Biotelemetry*, 1(20), 1–16. <https://doi.org/10.1186/2050-3385-1-20>
- Byrnes, E. E., Lear, K. O., Brewster, L. R., Whitney, N. M., Smukall, M. J., Armstrong, N. J., & Gleiss, A. C. (2021). Accounting for body mass effects in the estimation of field metabolic rates from body acceleration. *The Journal of Experimental Biology*, 224, jeb.233544. <https://doi.org/10.1242/jeb.233544>
- Cade, D. E., Barr, K. R., Calambokidis, J., Friedlaender, A. S., & Goldbogen, J. A. (2018). Determining forward speed from accelerometer jiggle in aquatic environments. *Journal of Experimental Biology*, 221(2). <https://doi.org/10.1242/jeb.170449>
- Clark, C. J. (2009). Courtship dives of Anna's hummingbird offer insights into flight performance limits. *Proceedings of the Royal Society B: Biological Sciences*, 276(1670), 3047–3052. <https://doi.org/10.1098/rspb.2009.0508>
- Fish, F. E. (2002). Balancing requirements for stability and maneuverability in cetaceans. *Integrative and Comparative Biology*, 42, 85–93. <https://doi.org/10.1093/icb/42.1.85>
- Gleiss, A. C., Dale, J. J., Holland, K. N., & Wilson, R. P. (2010). Accelerating estimates of activity-specific metabolic rate in fishes: Testing the applicability of acceleration data-loggers. *Journal of Experimental Marine Biology and Ecology*, 385, 85–91. <https://doi.org/10.1016/j.jembe.2010.01.012>
- Gleiss, A. C., Gruber, S. H., & Wilson, R. P. (2009). Multi-channel data-logging: Towards determination of behaviour and metabolic rate in free-swimming sharks. In J. Nielsen, H. Arrizabalaga, N. Fragoso, A. Hobday, M. Lutcavage, & J. Sibert (Eds.), *Tagging and tracking of marine animals with electronic devices, Reviews: Methods and Technologies in Fish Biology and Fisheries* (Vol. 9, pp. 211–228). Springer. <https://doi.org/10.1007/978-1-4020-9640-2>
- Gleiss, A. C., Jorgensen, S. J., Liebsch, N., Sala, J. E., Norman, B., Hays, G. C., Quintana, F., Grundy, E., Campagna, C., Trites, A. W., Block, B. A., & Wilson, R. P. (2011). Convergent evolution in locomotory patterns of flying and swimming animals. *Nature Communications*, 2, 352. <https://doi.org/10.1038/ncomms1350>
- Gleiss, A. C., Norman, B., & Wilson, R. P. (2011). Moved by that sinking feeling: Variable diving geometry underlies movement strategies in whale sharks. *Functional Ecology*, 25, 595–607. <https://doi.org/10.1111/j.1365-2435.2010.01801.x>
- Gleiss, A. C., Wilson, R. P., & Shepard, E. L. C. (2011). Making overall dynamic body acceleration work: On the theory of acceleration as a proxy for energy expenditure. *Methods in Ecology and Evolution*, 2, 23–33. <https://doi.org/10.1111/j.2041-210X.2010.00057.x>
- Gough, W. T., Segre, P. S., Bierlich, K. C., Cade, D. E., Potvin, J., Fish, F. E., Dale, J., di Clemente, J., Friedlaender, A. S., Johnston, D. W., Kahane-Rapport, S. R., Kennedy, J., Long, J. H., Oudejans, M., Penry, G., Savoca, M. S., Simon, M., Videsen, S. K. A., Visser, F., ... Goldbogen, J. A. (2019). Scaling of swimming performance in baleen whales. *The Journal of Experimental Biology*, jeb.204172. <https://doi.org/10.1242/jeb.204172>
- Halsey, L. G. (2017). Relationships grow with time: A note of caution about energy expenditure-proxy correlations, focussing on accelerometry as an example. *Functional Ecology*, 31(6), 1176–1183. <https://doi.org/10.1111/1365-2435.12822>
- Halsey, L. G., Green, J. A., Wilson, R. P., & Frappell, P. B. (2009). Accelerometry to estimate energy expenditure during activity: Best practice with data loggers. *Physiological and Biochemical Zoology*, 82(4), 396–404. <https://doi.org/10.1086/589815>
- Johnson, M. P., Madsen, P. T., Zimmer, W. M. X., Aguilar de Soto, N., & Tyack, P. L. (2004). Beaked whales echolocate on prey. *Proceedings of the Royal Society of London. Series B: Biological Sciences*, 271(Suppl). <https://doi.org/10.1098/rsbl.2004.0208>
- Johnson, M. P., & Tyack, P. L. (2003). A digital acoustic recording tag for measuring the response of wild marine mammals to sound. *Journal of Oceanic Engineering*, 28(1), 3–12. <https://doi.org/10.1109/JOE.2002.808212>
- Kawabata, Y., Noda, T., Nakashima, Y., Nanami, A., Sato, T., Takebe, T., & Soyano, K. (2014). Use of a gyroscope/accelerometer data logger to identify alternative feeding behaviours in fish. *Journal of Experimental Biology*, 217, 3204–3208. <https://doi.org/10.1242/jeb.108001>
- Kilbourne, B. M., & Hoffman, L. C. (2013). Scale effects between body size and limb design in quadrupedal mammals. *PLoS One*, 8(11), e78392. <https://doi.org/10.1371/journal.pone.0078392>
- Ladds, M. A., Rosen, D. A. S., Slip, D. J., & Harcourt, R. G. (2017). Proxies of energy expenditure for marine mammals: An experimental test of 'the time trap'. *Scientific Reports*, 7(11815), 1–10. <https://doi.org/10.1038/s41598-017-11576-4>
- Le Boeuf, B. J., Naito, Y., Asaga, T., Crocker, D., & Costa, D. P. (1992). Swim speed in a female northern elephant seal: Metabolic and foraging implications. *Canadian Journal of Zoology*, 70(4), 786–795. <https://doi.org/10.1139/z92-111>
- Lighthill, M. J. (1971). Large-amplitude elongated-body theory of fish locomotion. *Proceedings of the Royal Society of London B: Biological Sciences*, 179(1055), 125–138.
- Lindsey, C. C. (1978). Form, function and locomotory habits in fish. In W. S. Hoar & D. J. Randall (Ed.), *Fish physiology* (Vol. VII, pp. 1–100). Academic Press.
- Martín López, L. M., Aguilar de Soto, N., Madsen, P. T., & Johnson, M. P. (2021). Data from: Overall dynamic body acceleration measures activity differently on large vs small aquatic animals. *Dryad Digital Repository*, <https://doi.org/10.5061/dryad.ns1rn8p8rc>
- Martín López, L. M., Aguilar de Soto, N., Miller, P. J. O., & Johnson, M. P. (2016). Tracking the kinematics of caudal-oscillatory swimming: A comparison of two on-animal sensing methods. *Journal of Experimental Biology*, 219, 2103–2109. <https://doi.org/10.1242/jeb.136242>
- Martín López, L. M., Miller, P. J. O., Aguilar de Soto, N., & Johnson, M. P. (2015). Gait switches in deep-diving beaked whales: Biomechanical strategies for long-duration dives. *Journal of Experimental Biology*, 218, 1325–1338. <https://doi.org/10.1242/jeb.106013>
- Medler, S. (2002). Comparative trends in shortening velocity and force production in skeletal muscles. *American Journal of Physiology - Regulatory Integrative and Comparative Physiology*, 283, 368–378. <https://doi.org/10.1152/ajpregu.00689.2001>
- Miller, P. J. O., Johnson, M. P., Tyack, P. L., & Terray, E. A. (2004). Swimming gaits, passive drag and buoyancy of diving sperm whales *Physeter macrocephalus*. *Journal of Experimental Biology*, 207, 1953–1967. <https://doi.org/10.1242/jeb.00993>
- Qasem, L., Cardew, A., Wilson, A., Griffiths, I., Halsey, L. G., Shepard, E. L. C., Gleiss, A. C., & Wilson, R. (2012). Tri-axial dynamic acceleration as a proxy for animal energy expenditure; should we be summing values or calculating the vector? *PLoS One*, 7(2), e31187. <https://doi.org/10.1371/journal.pone.0031187>
- Saadat, M., Fish, F. E., Domel, A. G., Di Santo, V., Lauder, G. V., & Haj-Hariri, H. (2017). On the rules for aquatic locomotion. *Physical Review Fluids*, 2(8), 1–12. <https://doi.org/10.1103/PhysRevFluids.2.083102>
- Sato, K., Watanuki, Y., Takahashi, A., Miller, P. J. O., Tanaka, H., Kawabe, R., Ponganis, P. J., Handrich, Y., Akamatsu, T., Watanabe, Y., Mitani, Y., Costa, D. P., Bost, C.-A., Aoki, K., Amano, M., Trathan, P., Shapiro, A., & Naito, Y. (2007). Stroke frequency, but not swimming speed, is related to body size in free-ranging seabirds, pinnipeds and

- cetaceans. *Proceedings of the Royal Society B: Biological Sciences*, 274(1609), 471–477. <https://doi.org/10.1098/rspb.2006.0005>
- Savage, P. G. (1998). Strapdown Inertial Navigation Integration algorithm design part 1: Attitude algorithms. *Journal of Guidance, Control and Dynamics*, 21(1), 19–28. Retrieved from <http://pdf.aiaa.org/jaPreView/JGCD/1998/PVJAIMP4228.pdf>
- Schmidt-Nielsen, K. (1972). Locomotion: Energy cost of swimming, flying, and running. *American Association for the Advancement of Science*, 177(4045), 222–228.
- Schmidt-Wellenburg, C. A., Engel, S., & Visser, G. H. (2008). Energy expenditure during flight in relation to body mass: Effects of natural increases in mass and artificial load in Rose Coloured Starlings. *Journal of Comparative Physiology B*, 178, 767–777. <https://doi.org/10.1007/s00360-008-0267-7>
- Shepard, E., Wilson, R. P., Halsey, L. G., Quintana, F., Gómez Laich, A., Gleiss, A. C., Liebsch, N., Myers, A. E., & Norman, B. (2008). Derivation of body motion via appropriate smoothing of acceleration data. *Aquatic Biology*, 4, 235–241. <https://doi.org/10.3354/ab00104>
- Shiomi, K., Narazaki, T., Sato, K., Shimatani, K., Arai, N., Ponganis, P. J., & Miyazaki, N. (2010). Data-processing artefacts in three-dimensional dive path reconstruction from geomagnetic and acceleration data. *Aquatic Biology*, 8, 299–304. <https://doi.org/10.3354/ab00239>
- Simon, M. J., Johnson, M. P., & Madsen, P. T. (2012). Keeping momentum with a mouthful of water: Behavior and kinematics of humpback whale lunge feeding. *Journal of Experimental Biology*, 215, 3786–3798. <https://doi.org/10.1242/jeb.071092>
- Taylor, R. C., Schmidt-nielsen, K., & Raab, J. L. (1970). Scaling of energetic cost of running to body size in mammals. *The American Journal of Physiology*, 219(4), 1104–1107. <https://doi.org/10.1152/ajplegacy.1970.219.4.1104>
- Tucker, V. A. (1970). Energetic cost of locomotion in animals. *Comparative Biochemistry and Physiology - Part A: Molecular & Integrative Physiology*, 34, 841–846. [https://doi.org/10.1016/0010-406X\(70\)91006-6](https://doi.org/10.1016/0010-406X(70)91006-6)
- Tyack, P. L., Zimmer, W. M. X., Moretti, D., Southall, B. L., Claridge, D. E., Durban, J. W., Clark, C. W., D'Amico, A., DiMarzio, N., Jarvis, S., McCarthy, E., Morrissey, R., Ward, J., & Boyd, I. L. (2011). Beaked whales respond to simulated and actual navy sonar. *PLoS One*, 6(3), e17009. <https://doi.org/10.1371/journal.pone.0017009>
- Ware, C., Trites, A. W., Rosen, D. A. S., & Potvin, J. (2016). Averaged propulsive body acceleration (APBA) can be calculated from biologging tags that incorporate gyroscopes and accelerometers to estimate swimming speed, hydrodynamic drag and energy expenditure for Steller sea lions. *PLoS One*, 11(6), e0157326. <https://doi.org/10.1371/journal.pone.0157326>
- Williams, H. J., Holton, M. D., Shepard, E. L. C., Largey, N., Norman, B., Ryan, P. G., Duriez, O., Scantlebury, M., Quintana, F., Magowan, E. A., Marks, N. J., Alagaili, A. N., Bennett, N. C., & Wilson, R. P. (2017). Identification of animal movement patterns using tri-axial magnetometry. *Movement Ecology*, 5(6), 1–14. <https://doi.org/10.1186/s40462-017-0097-x>
- Williams, T. M. (1999). The evolution of cost efficient swimming in marine mammals: Limits to energetic optimization. *Philosophical Transactions of the Royal Society of London B: Biological Sciences*, 354, 193–201.
- Wilson, R. P., Börger, L., Holton, M. D., Scantlebury, D. M., Gómez-Laich, A., Quintana, F., Rosell, F., Graf, P. M., Williams, H., Gunner, R., Hopkins, L., Marks, N., Gherardi, N. R., Duarte, C. M., Scott, R., Strano, M. S., Robotka, H., Eizaguirre, C., Fahlman, A., & Shepard, E. L. C. (2020). Estimates for energy expenditure in free-living animals using acceleration proxies; a reappraisal. *Journal of Animal Ecology*, 89(1), 161–172. <https://doi.org/10.1111/1365-2656.13040>
- Wilson, R. P., White, C. R., Quintana, F., Halsey, L. G., Liebsch, N., Martin, G. R., & Butler, P. J. (2006). Moving towards acceleration for estimates of activity-specific metabolic rate in free-living animals: The case of the cormorant. *Journal of Animal Ecology*, 75, 1081–1090. <https://doi.org/10.1111/j.1365-2656.2006.01127.x>
- Wisniewska, D. M., Johnson, M., Teilmann, J., Rojano-Doñate, L., Shearer, J., Sveegaard, S., Miller, L. A., Siebert, U., & Madsen, P. T. (2016). Ultra-high foraging rates of harbor porpoises make them vulnerable to anthropogenic disturbance. *Current Biology*, 26, 1441–1446. <https://doi.org/10.1016/j.cub.2016.03.069>

SUPPORTING INFORMATION

Additional supporting information may be found in the online version of the article at the publisher's website.

How to cite this article: Martín López, L. M., Aguilar de Soto, N., Madsen, P. T., & Johnson, M. (2022). Overall dynamic body acceleration measures activity differently on large versus small aquatic animals. *Methods in Ecology and Evolution*, 13, 447–458. <https://doi.org/10.1111/2041-210X.13751>